Infection and Drug Resistance

Dovepress
Taylor & Francis Group

Open Access Full Text Article

ORIGINAL RESEARCH

Single-Cell Multi-Omics Deciphers Core Gene Networks and Immune Interaction Collapse in Sepsis-Associated T Cell Dysfunction

Xiang Li, Zhibin Chen, Yandong Yao, Muhu Chen, Yingchun Hu

Department of Emergency Medicine, The Affiliated Hospital, Southwest Medical University, Luzhou, 646000, People's Republic of China

Correspondence: Muhu Chen; Yingchun Hu, Email cmh6186@swmu.edu.cn; huyingchun913@swmu.edu.cn

Introduction: Sepsis is a life-threatening condition characterized by immune dysregulation, yet the mechanisms underlying T cell dysfunction remain poorly understood.

Methods: We integrated multi-omics data from public GEO datasets and prospective cohorts. Single-cell transcriptomic analysis was applied to identify core genes, followed by diagnostic and prognostic validation. Cell–cell interaction networks were constructed to investigate signaling alterations, and cross-platform validation was conducted.

Results: Seven core genes (*LTB, CD3D, TRAF3IP3, CD3G, GZMM, HLA-DPB1, CD3E*) were identified, showing strong diagnostic value (AUC ≥ 0.86) and prognostic significance (HR=4.50 for *CD3E*). Network analysis revealed collapse of critical signaling axes (HLA-DRA-MHCII, ITGB2-CD226) and aberrant activation of inhibitory pathways (LGALS9-CD45), leading to a "co-stimulation inhibition–checkpoint activation" imbalance. Cross-platform validation confirmed conserved downregulation of these genes in sepsis, which contributed to immune exhaustion via disrupted T cell differentiation trajectories and impaired intercellular communication.

Conclusion: Our findings highlight novel biomarkers and potential therapeutic targets for sepsis immunotherapy by systematically deciphering core gene networks and immune interaction collapse in T cell dysfunction.

Keywords: sepsis, single-cell rna sequencing, t cell exhaustion, biomarkers, cell-cell communication

Introduction

Sepsis remains a critical global health challenge, causing over 10 million annual deaths through its hallmark triad of infection-induced host response dysregulation, immune homeostasis disruption, and progressive organ failure.[1,2] While conventional biomarkers like C-reactive protein (CRP) and procalcitonin (PCT) have established utility in infection monitoring,[3] they fail to adequately characterize sepsis-specific immunopathological mechanisms, thereby limiting their prognostic value and therapeutic relevance. Recent studies have highlighted the promise of emerging non-invasive biomarkers, particularly microRNAs, which have demonstrated diagnostic and prognostic potential in neonatal sepsis—for example, miR-1, miR-124, and miR-34a showed high specificity and predictive value.[4] The advent of transformative technologies including single-cell RNA sequencing (scRNA-seq) has fundamentally reshaped our understanding of sepsis immunobiology, enabling unprecedented resolution of immune cell heterogeneity and regulatory dynamics.[5,6] Emerging evidence indicates that dynamic phenotypic remodeling in circulating T lymphocytes correlates strongly with disease severity gradients and treatment responsiveness, yet the upstream molecular drivers orchestrating these cellular transformations, particularly their microenvironment-modulating effects, await systematic elucidation.[7,8]

Single-cell sequencing technology has fundamentally advanced our understanding of functionally distinct cellular subsets in complex pathologies through high-resolution transcriptomic profiling, with transformative applications spanning from tumor ecosystems to autoimmune disorders.[9–11] In sepsis research, seminal work by Reyes et al uncovered profound tissue-wide remodeling of peripheral immunity using scRNA-seq, establishing cellular-scale molecular dysregulation as a key determinant of immunosuppressive conversion.[12] Of particular clinical relevance, T-cell dysfunction, often described as exhaustion-like

Received: 7 May 2025
Accepted: 7 September 2025
Published: 13 September 2025

Graphical Abstract

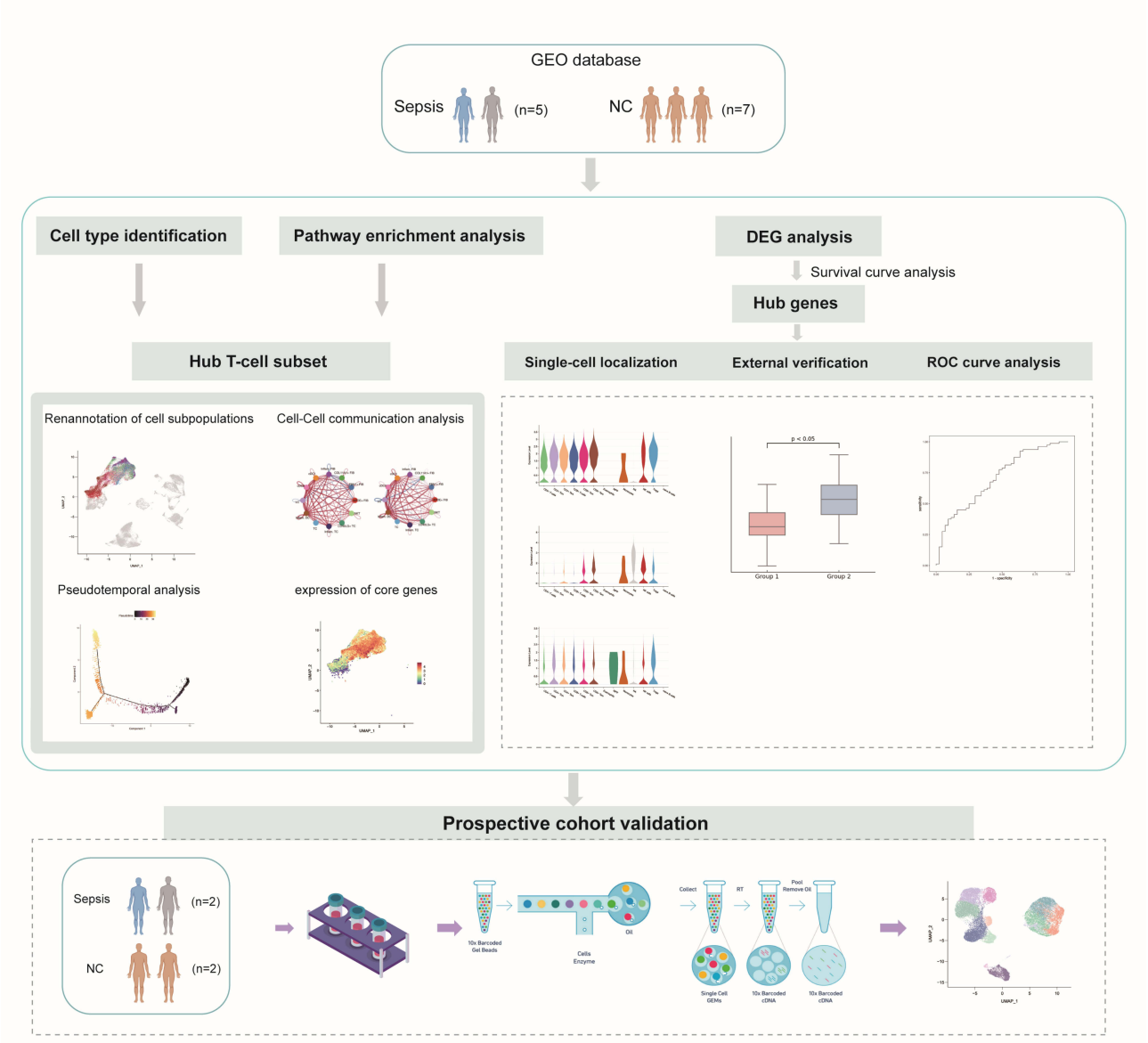

phenotypes (eg, effector function impairment and potential upregulation of immune checkpoints such as PD-1), has been proposed as a key mechanism of adaptive immunity failure and a predictor of poor prognosis in sepsis.[13,14] However, current studies still lack a systematic screening of key driver genes involved in T cell dysfunction, and the mechanisms by which these genes regulate intercellular interaction networks—such as signaling pathway crosstalk between T cells and monocytes—to influence immune microenvironmental dysregulation remain unclear. This knowledge gap hampers the development of targeted therapeutic strategies based on T cell functional remodeling.

Our results align along a continuous chain of evidence: First, genome-wide GSEA on GSE167363 and GSE220189 revealed an overarching pattern of upregulated innate immunity with suppressed T-cell programs. Next, single-cell differential and GO analyses narrowed this imbalance to TCR signaling and MHC-II antigen presentation. Within this framework, survival analyses in GSE65682 (n=478) identified seven core genes (*LTB, CD3D, TRAF3IP3, CD3G, GZMM, HLA-DPB1, CD3E*) significantly associated with prognosis. These genes localized to T-cell–related lineages in the single-cell

atlas and aligned with impaired co-stimulatory, antigen-presentation, and inhibitory axes in the CellPhoneDB/CellChat interaction maps. Pseudotime (Monocle3) then showed concordant temporal downtrends along T-cell state transitions (toward functionally impaired states, without making a definitive "exhaustion" claim). Finally, we conducted multi-layer validation in an independent prospective cohort (bulk RNA: sepsis=22, controls=10; scRNA-seq: two sepsis–control pairs) and in external datasets (ROC in GSE95233; expression differences in GSE232753, GSE69063, GSE185263, GSE100159), supporting translational potential. Importantly, bulk RNA survival analysis further demonstrated significantly elevated 28-day mortality in low-expression groups of *CD3D* (72.7% vs high-expression group, HR=3.25, 95% CI 1.02–10.34, p=0.046) and *CD3E* (75.0% vs high-expression group, HR=4.50, 95% CI 1.30–15.54, p=0.017). Together, this study establishes a multi-level evidence chain linking single-cell interaction networks to clinical outcomes, providing novel insights for sepsis biomarker development and therapies targeting immune microenvironment dysregulation (Figure 1).

Materials and Methods

Data Sources and Availability

The present study utilized both publicly available datasets and prospectively generated sequencing data. Publicly accessible datasets were retrieved from the Gene Expression Omnibus (GEO, https://www.ncbi.nlm.nih.gov/geo/), including:

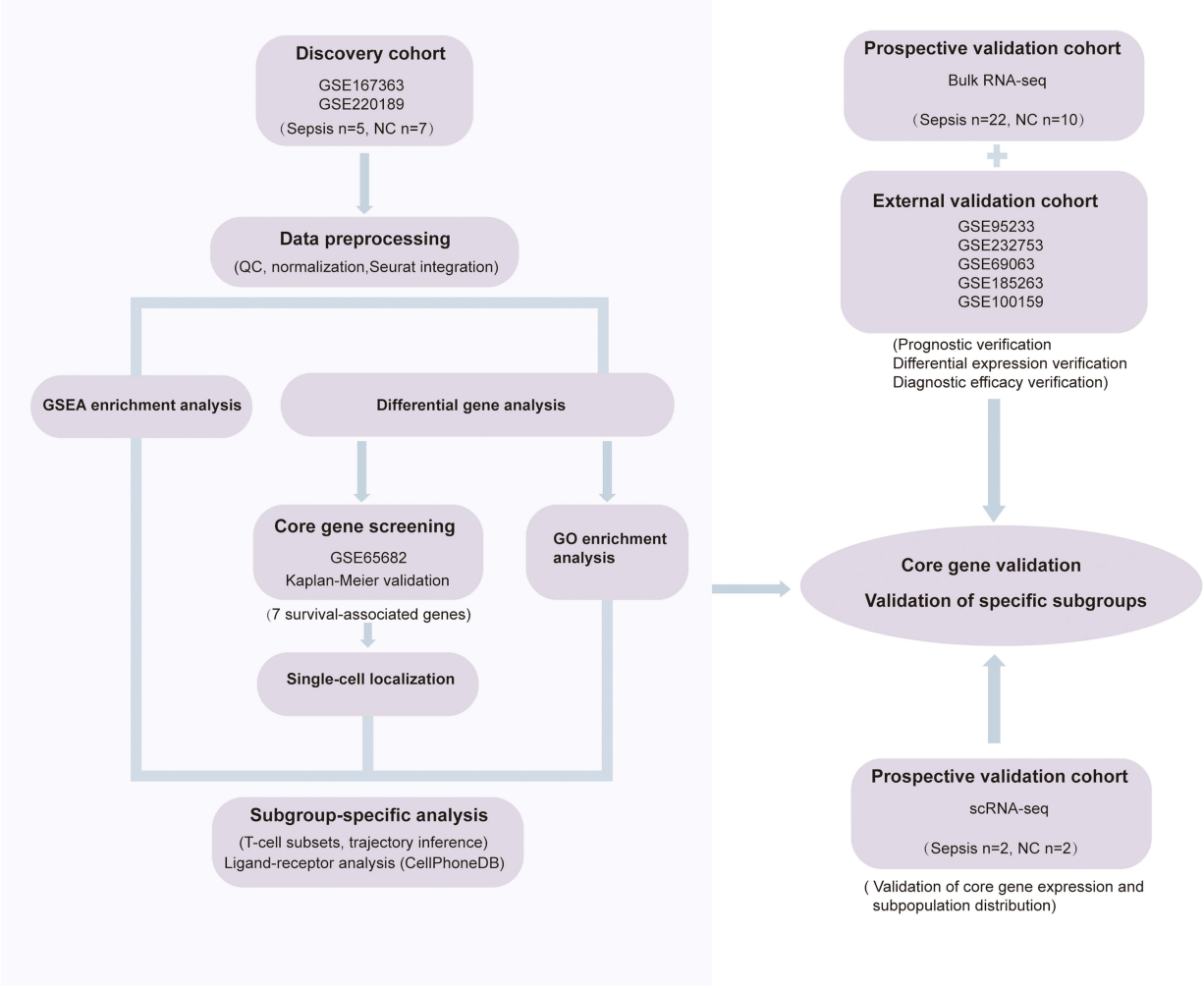

Figure 1 Summary of the single-cell sequencing analysis process. This study initially integrated single-cell sequencing datasets from the public GEO database. Through rigorous quality control (Harmony-based dimensionality reduction), differential gene expression analysis ($|log2FC| \geq 1.5$, $p < 0.05$), and functional enrichment analyses (GO/GSEA), seven core genes significantly associated with sepsis survival were identified. By combining single-cell localization, single-cell communication analysis (CellPhoneDB), and differentiation trajectory modeling (Monocle3), the molecular mechanisms underlying T cell subset dysfunction were systematically elucidated. Cross-platform validation using prospective bulk-RNA datasets and GEO datasets further confirmed the diagnostic potential of the core genes. Finally, prospective cohort single-cell transcriptomic data revealed a consistent downregulation of these core genes and a collapse of interaction networks within T cell subsets, offering novel diagnostic biomarkers and therapeutic targets for sepsis.

1. Two single-cell RNA sequencing (scRNA-seq) datasets:

- GSE167363 (GPL24676 platform): Comprising peripheral blood mononuclear cells (PBMCs) from 5 septic patients (3 survivors, 2 non-survivors) and 2 healthy controls.
- GSE220189 (GPL30173 platform): Containing PBMC profiles of 5 healthy donors.

2. Six bulk RNA sequencing datasets: GSE65682, GSE232753, GSE95233, GSE69063, GSE185263, and GSE100159, covering diverse clinical cohorts encompassing both sepsis patients and healthy controls.

Complementing these public resources, we integrated original multi-omics data generated through our institutional research program[15–18] (CNGBdb accession: CNP0002611; https://db.cngb.org/):

Bulk RNA sequencing data from a prospective cohort of 22 sepsis patients and 10 healthy controls.

scRNA-seq profiles of 2 septic patients (1 survivor, 1 non-survivor) and 2 matched controls.

For clarity, all datasets were categorized into specific cohorts as summarized in Supplementary Table 1. Specifically, GSE167363 and GSE220189 were designated as discovery cohorts for the identification of immune cell clusters and T cell subsets in scRNA-seq analyses. The prospective cohort (CNGBdb accession: CNP0002611) included 4 scRNA-seq samples for independent validation of clustering and marker genes, and 32 bulk RNA-seq samples for validation of hub genes and prognostic stratification. External validation was performed with multiple datasets: GSE65682 for hub gene validation and survival analysis, GSE95233 for ROC curve analysis, and GSE232753, GSE69063, GSE185263, and GSE100159 for independent validation of hub gene expression.

Prospective Cohort Specifications

This study was conducted with approval from the Ethics Committee of the Affiliated Hospital of Southwest Medical University (No. ky2018029) and registered at the Chinese Clinical Trial Registry (ChiCTR1900021261), in accordance with the Declaration of Helsinki. All participants provided written informed consent. The cohort was established following SEP-3 diagnostic criteria with detailed clinical characterization (Supplementary Table 2). Clinical variables captured included infection site and type (microbiology), SOFA score, PCT, lactate, leukocyte counts and differentials, and the 28-day outcome. Peripheral blood samples from 22 sepsis patients and 10 healthy controls were collected within 24 hours of diagnosis. RNA extraction and library preparation followed standardized protocols (TRIzol/NEBNext Ultra II). Notably, 2 randomly selected sepsis-control pairs underwent additional 10x Genomics-based scRNA-seq analysis. In the scRNA-seq subset (n=4), the two sepsis patients comprised one survivor and one non-survivor.

Cell Ranger Analysis

Single-cell transcriptomes were processed using Cell Ranger (10x Genomics v8.0.1), which identified cell barcodes and UMIs to quantify gene expression. The workflow automatically generated QC reports containing: (1) cell numbers (3,000–5,000 cells/sample); (2) median genes per cell; (3) sequencing depth (≥50,000 reads/cell); (4) saturation rates (>70%). Cell Ranger's automated pipeline converted raw data into FASTQ format and performed genome alignment (human GRCh38/mouse GRCm39). Technical details of UMI counting and gene-barcode matrices generation followed 10x Genomics' best practices.[19]

Gene Quantification Quality Control and Data Preprocessing

The Seurat package (version 4.0.0) was used for further quality control (QC) processing of the data. Most cells exhibit a concentrated distribution in terms of the number of expressed genes, UMI counts, and the proportion of mitochondrial transcript expression. Based on the distributions of key metrics such as nUMI, nGene, percent Mito, low-quality cells were filtered out. The specific quality control criteria were as follows:

- Cells with fewer than 200 detected genes were removed.
- Cells with fewer than 1,000 UMIs were excluded.
- Cells with log10GenesPerUMI values lower than 0.7 were filtered out.

- Cells with a mitochondrial UMI proportion greater than 30% were discarded.
- Cells with a hemoglobin gene proportion exceeding 5% were removed.

Additionally, DoubletFinder (version 2.0.3) was employed to identify and eliminate doublets before proceeding with downstream analysis. After completing the quality control process, the NormalizeData function was applied to normalize the data, ensuring consistency and comparability for subsequent analyses.

Cell Clustering and Marker Visualization

Marker gene identification was performed in Seurat (v4.3) with the FindAllMarkers function (presto test) followed by two visualization approaches: (1) violin plots for cell group distribution; (2) t-SNE projections for spatial expression patterns. Quality control ensured analysis of cells with 200–2500 detected genes and <15% mitochondrial content.

Cell Annotation and Differential Analysis

Cell types were annotated using SingleR (v1.4.1) through correlation matching by comparing target cells with reference data from the Human Primary Cell Atlas and selecting top-matched cell types based on a Spearman correlation coefficient (ρ) threshold >0.7. Differentially expressed genes were identified under strict criteria, requiring an adjusted *p*-value <0.05 (calculated via the Benjamini-Hochberg method) and an absolute log2 fold change (|log2FC|) >1.5. The entire analytical workflow was further validated using peripheral blood mononuclear cells isolated from healthy controls to ensure methodological robustness.

Functional Profiling of Differentially Expressed Genes

All protein-coding genes were used as the background, and the list of differentially expressed protein-coding genes was used as the candidate set for enrichment analysis. To determine the enrichment significance of GO terms, p-values were calculated using the hypergeometric distribution test and corrected by the Benjamini–Hochberg method for multiple testing. Gene Ontology (GO) and Gene Set Enrichment Analysis (GSEA) were performed using clusterProfiler (v4.4.2), with results visualized through ggplot2 in R, and results were visualized with the ggplot2 package in R.

Constructing Differential Gene Protein Networks

In this project, the differential gene sequences with top20 ploidy of difference were selected and compared with the protein sequences of the species in the STRING database by blast (e-value< 10–10) to obtain the interrelationships of the genes, from which the interactions of the differential genes were extracted, and the interactions were mapped on the interactions network by Cytoscape (3.10.1).

Survival Analysis

Genes were assessed for association with 28-day survival using the Kaplan-Meier method based on the GSE65682 dataset (n=478), with statistical significance defined as $P<0.05$ in the Log rank test.

For the 22 sepsis patients, the high expression group and low expression group were determined based on the median expression levels of each core gene. Kaplan-Meier method was used to assess the 28-day survival rate difference between the two groups, and the survival curves were compared using the Log rank test (with a significance threshold set at $P<0.05$). To further quantify the risk association, univariate Cox proportional hazards regression model was used to calculate the hazard ratio (HR) and its 95% confidence interval (CI).

Diagnostic Value of Core Genes

To further evaluate the diagnostic potential of the selected core genes in an independent sepsis cohort, the GSE95233 dataset (n=124) was analyzed. The receiver operating characteristic (ROC) curve was generated, and the area under the curve (AUC) was determined using the pROC package (v1.18.0).

External Validation

Our pre-collected RNA sequencing data (sepsis = 22 cases, normal controls = 10 cases) was utilized to compare core gene expression between the two groups. The results were visualized using R-generated box plots to confirm the differential expression of core genes in sepsis patients versus healthy individuals.

After homogenizing the datasets obtained from the GEO database (GSE232753, GSE69063, GSE185263, and GSE100159), the samples were classified into sepsis groups and normal control groups. To confirm differences in core gene expression between the sepsis and normal groups, a *t*-test was conducted for each gene within the same group across all datasets using R packages. This statistical analysis helped confirm whether the core genes exhibited significant differences in expression levels between the sepsis and normal groups.

Cell-Cell Interaction Network Analysis

CellChat is a computational framework designed to predict and analyze intercellular communication networks based on single-cell RNA sequencing (scRNA-seq) data. It integrates single-cell expression profiles with known ligands, receptors, and auxiliary factors (also referred to as heteromeric molecular complexes) to quantify the strength of cell-cell interactions. This approach overcomes the limitation of considering only individual ligand-receptor gene pairs, recognizing that many receptors function as multi-subunit complexes.[20]

The strength of cell-cell interactions among different subpopulations is assessed using a permutation test.[21] A ligand-receptor pair is considered significant in intercellular communication if it meets the following criteria: (i) an interaction strength exceeding 10, and (ii) a p-value less than 0.01. These stringent criteria ensure the identification and analysis of only the most biologically relevant cell-cell signaling interactions.

Pseudotime Analysis

In this study, the Monocle package (v3) was used to apply machine learning algorithms based on key gene expression patterns, enabling the reconstruction of dynamic developmental trajectories over time.[22] The analytical workflow consists of the following steps:

- Selection of highly variable genes – Genes displaying significant expression variability across cells were identified.
- Dimensionality reduction – The expression profiles of these genes were subjected to spatial dimensionality reduction.
- Construction of a Minimum Spanning Tree (MST) – An MST was constructed to model the developmental trajectory.
- Identification of the longest path – The longest path within the MST was identified, representing the differentiation trajectory of transcriptionally similar cells.

Statistical Methods

Unless otherwise specified, all statistical and bioinformatics analyses in this study were performed using R software (v4.4.2) and GraphPad Prism (v10.0). Differential expression analyses of single-cell transcriptomes were conducted with the presto test in the Seurat package (based on the Wilcoxon rank-sum test), with *p*-values adjusted by the Benjamini–Hochberg method. Gene enrichment analyses (GO, GSEA) were evaluated using hypergeometric or permutation tests, with false discovery rate (FDR) correction applied. Survival analyses were carried out with the Kaplan–Meier method and Log rank test, supplemented by Cox proportional hazards regression to estimate hazard ratios (HRs) and 95% confidence intervals. Group comparisons of gene expression were performed using two-tailed Student's *t*-tests or Wilcoxon rank-sum tests as appropriate. Comparisons of immune cell proportions between groups were conducted using the chi-square test. All reported p-values were two-sided, and statistical significance was defined as $*p < 0.05$, $**p < 0.01$, and $***p < 0.001$.

Results

Quality Control of Single-Cell Sequencing Data

Single-cell transcriptome sequencing was performed on 12 biological samples (sepsis=5, controls=7) derived from datasets GSE167363 and GSE220189.After quantification and preliminary quality control (QC) analysis using Cell

Ranger (v8.0.1), the initial distribution of high-quality pre-filtered cells across samples ranged from 2,716 to 9,485. Next, a rigorous three-stage QC process was implemented: (i) Low-quality cell removal – Cells were filtered based on dual-threshold criteria (gene count < 200, UMI count < 1,000, log10GenesPerUMI < 0.7). (ii) Biological quality filtering – Apoptotic cells and red blood cell contamination were removed based on mitochondrial gene expression proportion > 30% and hemoglobin gene expression proportion > 5%. (iii) Doublet and multicell detection – Potential doublets and multicell aggregates were identified and removed using the machine learning algorithm DoubletFinder ($\alpha = 0.05$), excluding cells with pANN values > 0.9. Following systematic QC filtering, the final number of high-quality cells ranged from 2197 to 8676 (Supplementary Table 3).

To comprehensively assess the effectiveness of the QC process, key quality metrics, including nGene (number of detected genes per cell), nUMI (total UMI count per cell), and log10GenesPerUMI (log-transformed UMI-to-gene ratio), were visualized using violin plots (Supplementary Figure 1). Additionally, the distribution patterns of percent Mito (mitochondrial gene proportion) and percent HB (hemoglobin gene proportion) were analyzed to further validate data quality.

Dimensionality Reduction and Clustering Analysis

To mitigate the impact of technical variation across samples, the Harmony algorithm was first applied for batch effect correction.[23] Using the corrected high-dimensional data, nonlinear dimensionality reduction was performed via the Uniform Manifold Approximation and Projection (UMAP) algorithm, with the resolution set to 0.4. As shown in Figure 2A, a total of 22 distinct cell subpopulations exhibiting significant transcriptomic heterogeneity were identified.

By constructing a comprehensive cellular atlas, we systematically compared the sepsis group (SEPSIS) and the normal control group (NC) to uncover intergroup differences. The UMAP projection (Figure 2B) revealed that while cells from both groups exhibited a mixed distribution, partially discrete clustering patterns were observed in low-dimensional space, suggesting heterogeneous effects of disease state on cellular composition. These quantitative variations were further visualized using a spatial distribution map (Figure 2C), which highlighted significant intergroup shifts in key subpopulations, including cluster 2 (T-cell subpopulation), cluster 7 (NK-cell subpopulation), cluster 10 (monocytes), and cluster 17 (neutrophils).

Additionally, Figure 2D illustrates the proportional distribution of cells in different clusters between the sepsis and normal control groups. Notably, the relative abundance of specific cell populations differed significantly between groups, suggesting that sepsis may lead to immune system dysregulation by altering the composition of key immune cell subsets.

Characterization of the Immune Microenvironment in Sepsis

To further characterize the immune microenvironment in sepsis, UMAP projection was integrated with cell type-specific marker gene expression (Supplementary Table 4) to classify immune cell subsets. This approach identified six major immune cell types (Figure 2E): B lymphocytes ($CD79A^+$), monocytes ($CD68^+/CD163^+$), natural killer (NK) cells ($NCAM1^+/GNLY^+$), neutrophils ($S100A8^+/S100A9^+$), platelets ($PPBP^+$), and T lymphocytes ($CD2^+/TRAC^+$).

Comparative analysis showed a significant decrease in the proportion of T cells (47.4% vs 30.1%, $p<0.05$, chi-square test) and a significant increase in the proportion of neutrophils (0.19% vs 3.73%, $p<0.05$) in the sepsis group (Figure 2F). This characteristic pattern of lymphocyte reduction with myeloid expansion coincides with the phenomenon of imbalance between the storm of inflammatory factors (SIRS) and compensatory anti-inflammatory response (CARS) that occurs during the pathological process of sepsis. Particular attention should be paid to the marked decrease in T-cell ratio in sepsis patients compared to the normal group, which may suggest a specific impairment of cellular immune function.

GSEA Enrichment Analysis

Genome-wide pathway enrichment analysis (GSEA, $p<0.05$) performed across all single-cell transcriptomes from GSE167363 and GSE220189 revealed fundamental immune dysregulation in sepsis through bidirectional pathway polarization. Sepsis samples exhibited simultaneous hyperactivation of innate immunity networks and coordinated T cell dysfunction.

The neutrophil-centric activation signature dominated regulatory modules, encompassing granulocyte chemotaxis (NES= 2.55), platelet α-granule secretion (NES=2.71), and wound healing-associated ECM remodeling (NES=2.36) (Figure 3A). This promigratory phenotype coincided with paradoxical induction of tissue repair programs despite systemic tissue injury.

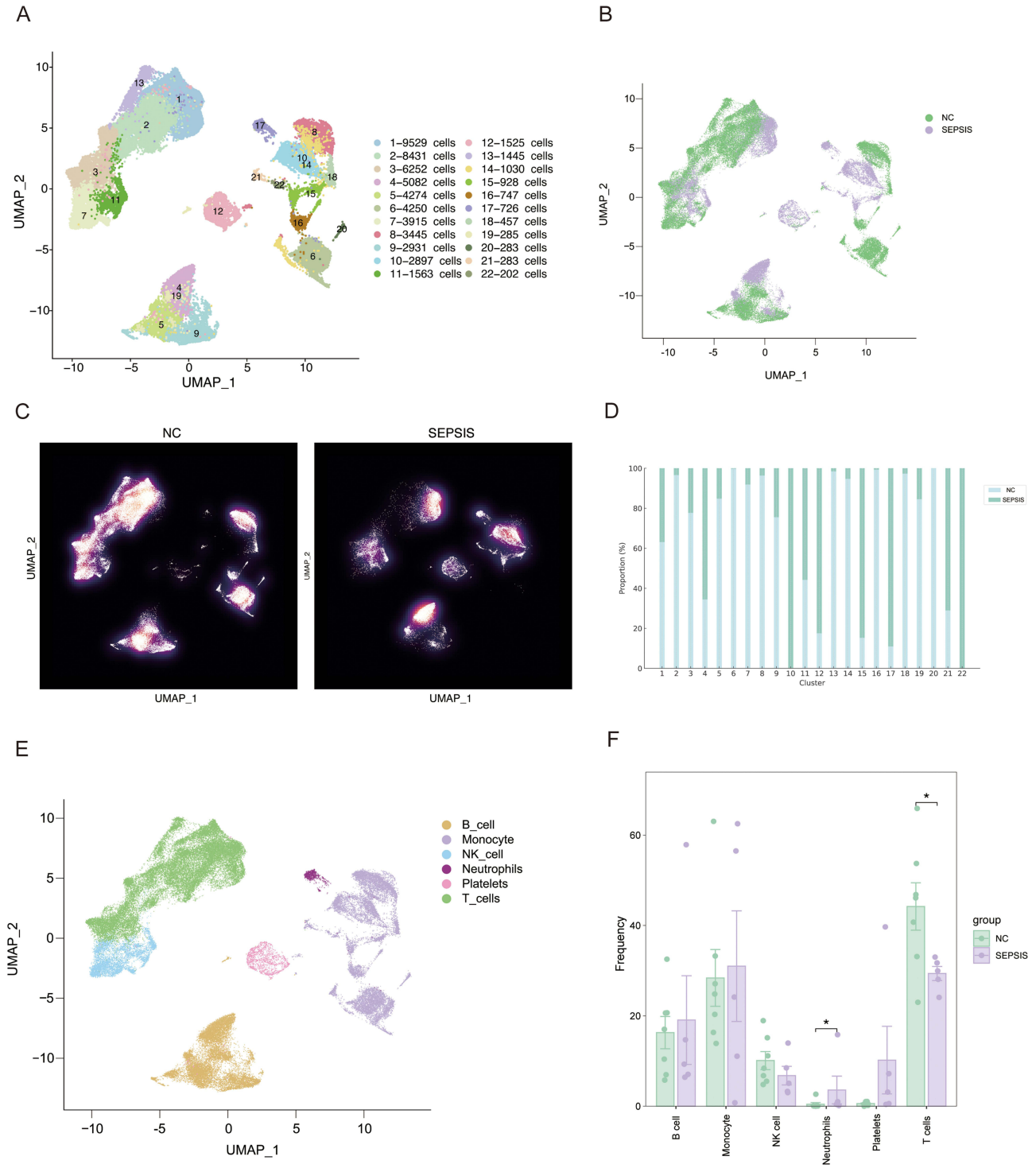

Figure 2 Sepsis peripheral blood cell landscape based on scRNA-seq datasets GSE167363 and GSE220189. (**A**) UMAP embedding identifies 22 distinct clusters (n = 60,480 single cells). Cluster annotation: T cells (C1, C2, C3, C13), B cells (C4, C5, C9, C19), NK cells (C7, C11), platelets (C12), neutrophils (C17), and monocytes (C6, C8, C10, C14–C16, C18, C20–C22). (**B**) UMAP embedding of single cells from normal controls (NC, green) and sepsis patients (purple), demonstrating the overall distribution and separation of the two groups. (**C**) Density distribution maps of single-cell populations in NC (left) and sepsis (right), showing distinct spatial topology and differential cell abundance patterns between groups. (**D**) Proportion of NC and SEPSIS across Clusters, cluster abundance differentials (two-tailed Wilcoxon test) showing depletion of T-cell clusters (C1-3,13) and expansion of neutrophils (C17). (**E**) Canonical marker-based annotation: T cells (CD2+/TRAC+), B cells (CD79A$^+$), macrophages (CD68$^+$/CD163$^+$), NKs (NCAM1$^+$/GNLY$^+$), neutrophils (S100A8$^+$/S100A9$^+$), platelets (PPBP$^+$). (**F**) Systemic immune shift: 36.5% relative T cell loss (47.4%→30.1%, p=0.048) with 19.1-fold neutrophil elevation (0.19→3.73%, p=0.0303). *p < 0.05.

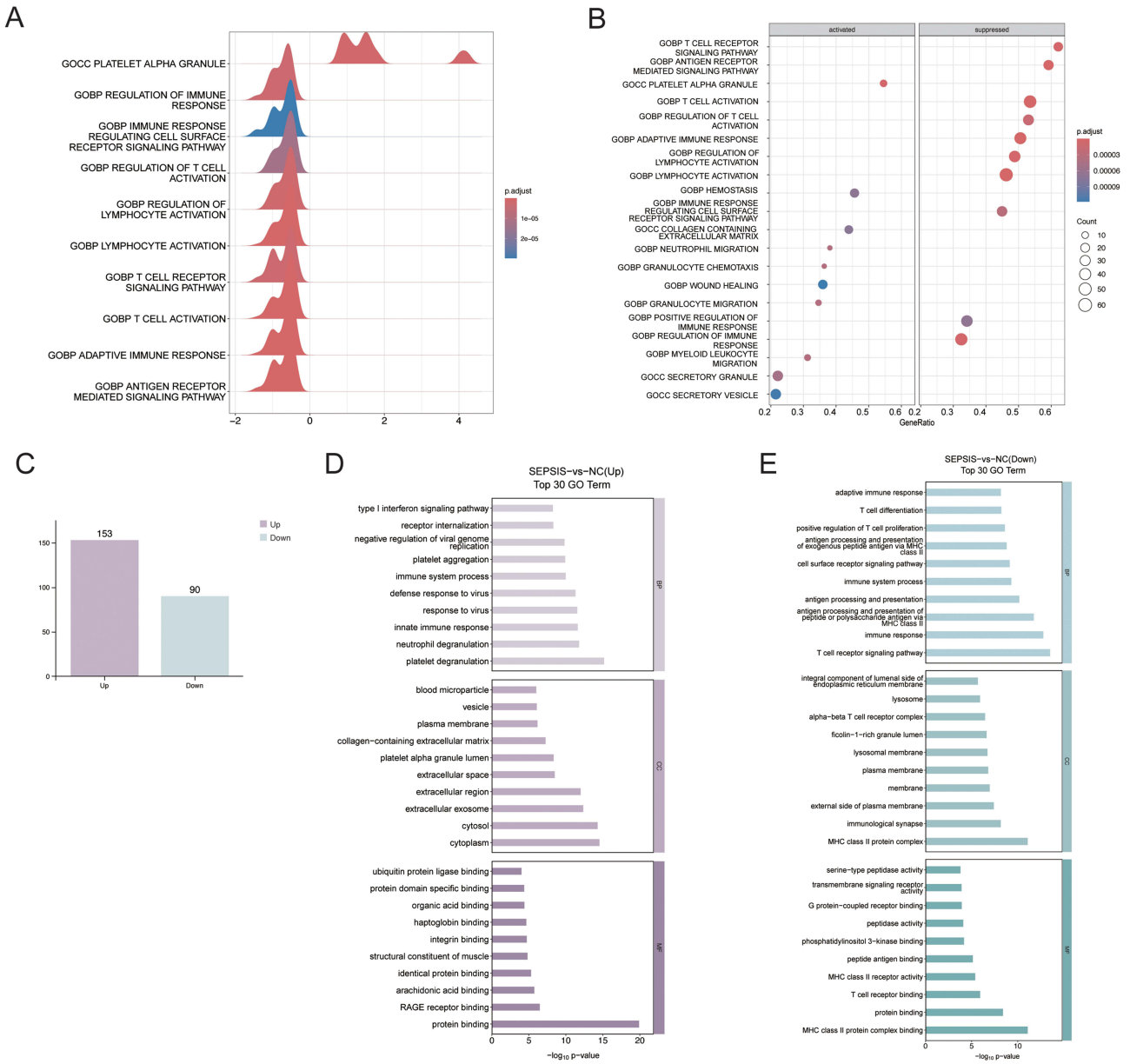

Figure 3 Functional enrichment and differential gene analysis of sepsis single-cell transcriptomes (GSE167363 and GSE220189). (**A**) Genome-wide gene set enrichment analysis (GSEA) performed across all single-cell transcriptomes from two scRNA-seq datasets (GSE167363 and GSE220189), showing the top 10 significantly enriched pathways. (**B**) Enrichment bubble plots of activated versus repressed pathways, with bubble size indicating Gene Ratio and color gradient reflecting p-values, adjust significance, showing significant pathways activated and repressed in the sepsis group compared to the normal group. (**C**) Significantly differentially expressed genes, showing 243 differentially expressed genes obtained by screening for multiplicity of differences (Fold Change > 1.5) and significance test ($p < 0.05$). 153 genes were up-regulated (purple) and 90 genes were down-regulated (light green) in the sepsis group. (**D**) Up-regulation of the top 30 GO pathways enriched for differential genes. (**E**) Downregulation of the top 30 GO pathways enriched for differential genes.

Parallel analysis demonstrated broad suppression of adaptive immunity effectors, particularly T cell receptor signaling (NES=−2.91) and lymphocyte activation modules (NES=−2.76) (Figure 3B).

The co-occurrence of myeloid hyperactivity and lymphocytic suppression demonstrates a mechanistic connection between granulocyte-mediated tissue damage and T-cell dysfunction/immune suppression. This dual-phase regulatory architecture suggests stratification potential for targeted intervention—neutrophil pathway modulation in acute stages followed by T cell reinvigoration during recovery. To further dissect the molecular pathways underlying this global pattern, we next conducted single-cell–level differential expression and functional annotation analyses.

https://doi.org/10.2147/IDR.S538883

Differential Gene Identification and GO Enrichment Analysis

Intergroup differential analysis was conducted across the whole single-cell transcriptome of 12 samples, using the presto algorithm (Seurat v4.0). A total of 243 differentially expressed genes (DEGs) were identified between sepsis patients and healthy controls (Supplementary Tables 5 and 6), among which 153 were significantly up-regulated and 90 were significantly down-regulated (screening criteria: $|\log2FC| \geq 1.5$ and adj. $p < 0.05$) (Figure 3C). Notably, the pathway convergence between these DEG-enriched features and prior GSEA results (Figure 3A and B) validated their systemic relevance while reinforcing analytical reproducibility.

Functional annotation analysis revealed significant biological patterns with up-regulated gene signatures: GO enrichment showed (Figure 3D) that DEGs in the sepsis group were mainly enriched in intrinsic immune activation-related pathways: (i) neutrophil degranulation (GO:0043312; p= 1.62E-12); (ii) innate immune response (GO:0045087; p=2.51E-12); (iii) defence response to virus (GO:0051607; p=5.02E-12), etc.

Down-regulated gene features: pathways related to T lymphocyte function showed systemic inhibition (Figure 3E), with the T cell receptor signalling pathway (GO:0050852; p= 3.21E-14, Enrichment score= 21.76077983) as the most significantly inhibited biological process, accompanied by positive regulation of T cell proliferation (GO:0042102; p= 2.47E-09) and significant downregulation of αβ-T cell receptor signalling pathway (GO:0042105; p= 3.46E-07). Key targets at the molecular-functional level were enriched in the MHC class II protein complex (GO:0042613; p=8.46E-12) and antigen presentation-associated activity (GO:0019886; p=1.60E-09).

Core Gene Screening and Identification

The top 20 significantly up- and down-regulated genes ($|\log2FC| \geq 1.5$) were selected to construct the expression heatmap (Figure 4A). Protein–protein interaction analysis was performed using the STRING database (version 11.5, confidence threshold >0.7), and the network was visualized in Cytoscape. The results showed that genes located at the central positions of the network were mainly enriched in the T-cell receptor complex and intrinsic immune regulation-related nodes (Figure 4B). Further validation in the sepsis clinical dataset GSE65682 (n=478) using Kaplan–Meier curves (Figure 4C–I) demonstrated that elevated expression of seven core genes (*LTB, CD3D, TRAF3IP3, CD3G, GZMM, HLA-DPB1*, and *CD3E*) was significantly associated with improved patient survival ($p < 0.05$), suggesting their potential value as prognostic biomarkers for sepsis.

Single-Cell Localization of Core Genes

Following the identification of seven survival-associated genes, we next mapped their lineage context in the single-cell atlas and assessed their correspondence with the dysregulated ligand–receptor axes. Single-cell resolution analysis identified six principal immune lineages through integrated dimensional reduction and Seurat-based cross-dataset harmonization (Figure 2E), with cell identities anchored to Human Cell Atlas-defined marker hierarchies: CD68+ monocytes/macrophages (clusters 6, 8, 10, 14, 15, 16, 18, 20, 21, 22), NCAM1+ natural killer cells (clusters 7,11), CD79A+ B lymphocytes (clusters 4,5,9,19), CD2+ T lymphocytes (clusters 1,2,3,13), alongside neutrophils (cluster 17) and platelets (cluster 12).

Spatial mapping of core sepsis-associated genes revealed lineage-restricted expression landscapes (Figure 5): *CD3D, CD3G*, and *CD3E* demonstrated T cell-specific dominance, while *LTB* exhibited dual localization in T and B lymphocytes. Cytotoxic effector *GZMM* partitioned between NK cells and T cell subsets, whereas *HLA-DPB1* exhibited preferential expression in B cells and NK populations, with fewer T cell involvement. *TRAF3IP3* displayed broad cellular distribution, prominently in monocytes and lymphoid lineages, indicative of its pleiotropic signaling roles.

Subclustering of T Cells and Overall Changes in the Interactions Network

Integrative analysis revealed critical involvement of T lymphocytes in sepsis progression through multi-modal evidence: (1) The observed 36.5% relative decrease in T cell proportions (47.4% → 30.1%, p=0.048) across sequenced cells; (2) pathway enrichment of differentially expressed genes for T cell activation/differentiation processes; (3) Intersection of single-cell-resolved localisation of core genes. Therefore, we subclustered and annotated T cells and identified 12 major subpopulations

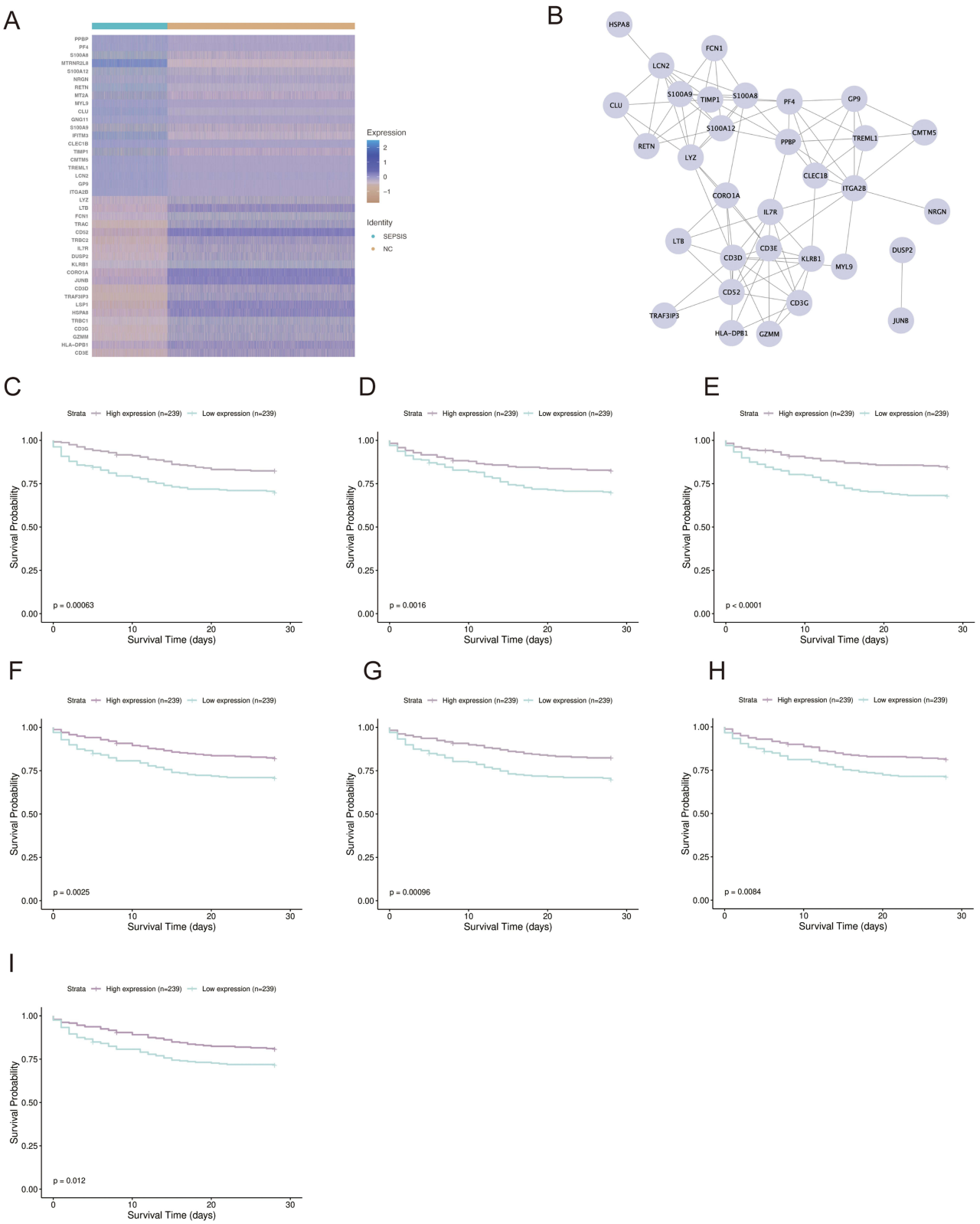

Figure 4 Systematic identification of sepsis core genes in single-cell genomes. (**A**) Heatmap of differential gene expression patterns, heatmap of up/down-regulated Top20 differential genes, row clustering for tracer gene expression signatures, column annotation for clinical grouping (blue: sepsis group, yellow: control group). Color gradients are defined: purple to high expression, yellow to low expression. (**B**) Topological resolution of protein interaction networks. (**C-I**) Kaplan-Meier curve validation (Log rank test) of survival prognosis for candidate genes based on dataset GSE65682. It shows that (**C**) *LTB* (**D**) *HLA-DPB1* (**E**) *TRAF3IP3* (**F**) *CD3D* (**G**) *GZMM* (**H**) *CD3E* (**I**) *CD3G*, and exhibit improved survival outcomes in the group with high expression at their gene level, ie, all of the above genes are protective genes.

https://doi.org/10.2147/IDR.S538883

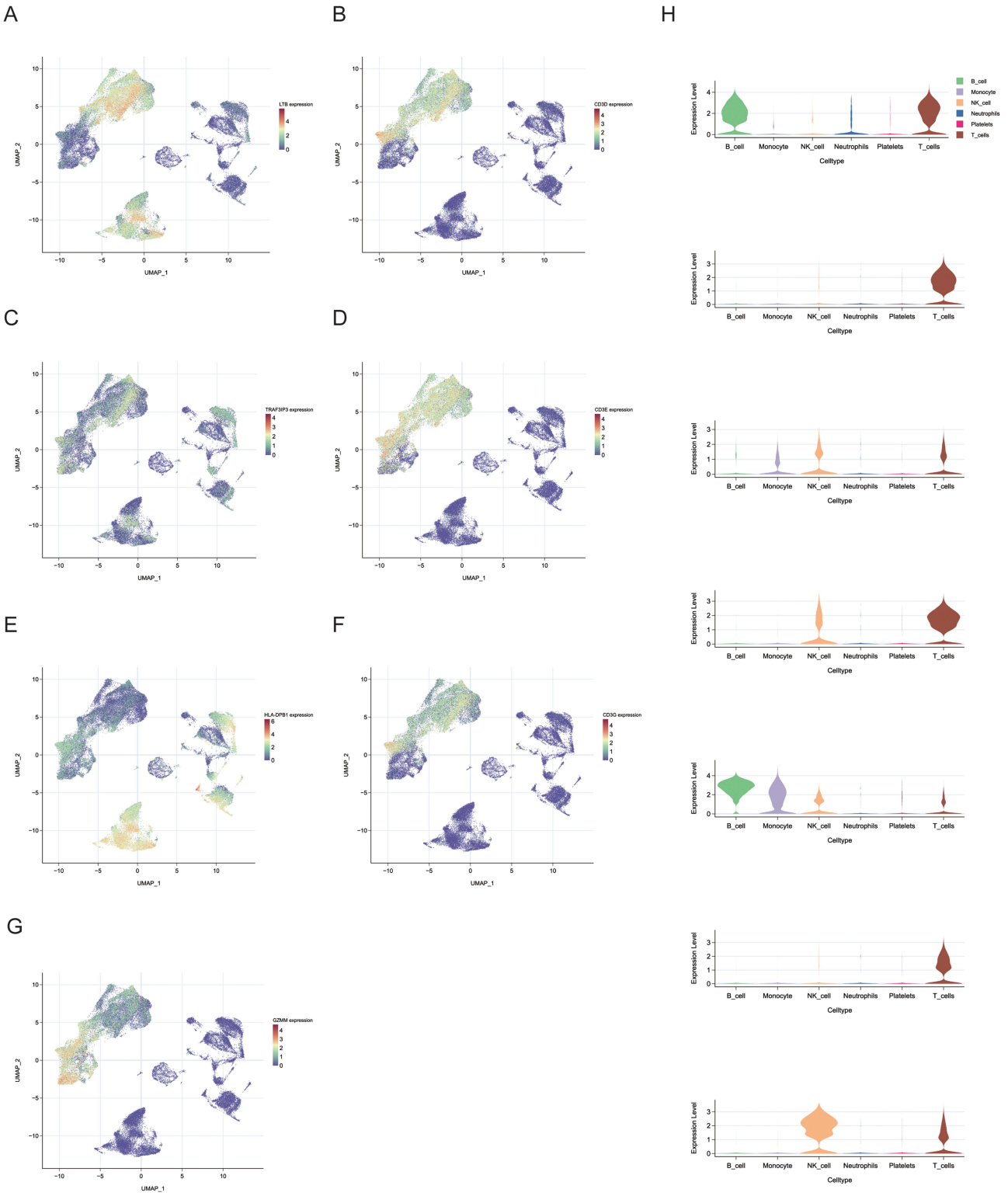

Figure 5 Single-cell localization of core genes. (**A**–**G**) Cellular localization of target genes, specifically (**A**) *LTB*, (**B**) *CD3D*, (**C**) *TRAF3IP3*, (**D**) *CD3E*, (**E**) *HLA-DPB1*, (**F**) *CD3G*, and (**G**) *GZMM*. (**H**) Violin plots of core gene expression across different cell types, arranged from top to bottom as *LTB, CD3D, TRAF3IP3, CD3E, HLA-DPB1, CD3G*, and *GZMM*.

(Figure 6A). Figure 6B demonstrates the differences in distribution and expression of these T cell subpopulations in the sepsis group (right) and the normal group (left), reflecting altered T cell immune tolerance or immunosuppressive status.

Cell-cell interaction mapping through CellPhoneDB revealed systemic collapse of T cell communication networks in sepsis. The frequency and intensity of interactions between T cells and other immune cells were markedly decreased compared to the controls ($p<0.01$) (Figure 6C), with inbound signaling deficits surpassing outbound reductions (Figure 6D and E), implying predominant loss of signal reception capacity. Critical cross-talk axes exhibited differential vulnerability: NK-T cell interactions; monocyte-T cell interactions; B-T cell collaboration in survival signaling exchange, etc.

Subgroup-Specific Changes in Key Ligand-Receptor Pairs

Comparative pathway analyses revealed that the T cell communication network was severely dysregulated during sepsis, characterized by collapsed antigen presentation, failure of inflammatory abatement and aberrant activation of inhibitory signaling axes. Among the antigen presentation mechanisms, MHC-II signaling (HLA-DRA-CD4) exhibited severe dysfunction. At the same time, activation of the pro-depletion signaling axis was evident, with sustained activation of the GALS9-CD45 and MIF-CD74 pathways driving T-cell depletion, while reduced ANXA1-FPR1 signaling similarly exacerbated the tissue damage-immune paralysis vicious cycle.

To further integrate the survival-derived core genes with the intercellular communication map, we mapped these genes onto the ligand–receptor network (Figure 6F). Several consistent patterns were observed. First, HLA-DPB1, as part of the MHC-II complex, corresponded to the attenuated antigen-presenting interactions with $CD4^+$ T cells (eg, HLA-DRA–CD4 and HLA-DPB1–CD4). Second, the TCR components *CD3D, CD3E*, and *CD3G*, although not directly forming ligand–receptor pairs, act downstream of these MHC-II–CD4 signals and thereby reflect the weakened antigen-presentation–to-TCR signaling axis. Third, *GZMM* did not appear as a ligand–receptor pair in CellPhoneDB/CellChat, but its downregulation was consistent with the reduced intensity of cytotoxic and NK–T cell interactions highlighted in the network. Finally, *LTB* and *TRAF3IP3* function mainly as regulators rather than direct communication ligands or receptors; although not represented in the interaction map under our thresholds, their decreased expression aligned with the overall pattern of impaired lymphoid organization and weakened regulatory modules. Together, these findings link the seven core genes to specific communication deficits, suggesting that diminished antigen presentation and co-stimulatory inputs converge on a less responsive TCR complex, accompanied by reduced cytotoxic output.

T Cell Differentiation Trajectory and Dynamic Expression of Core Genes

Through pseudotime analysis, we can uncover the developmental or differentiation processes of different T cell subpopulations in sepsis and investigate how target genes regulate T cell function at different time points or immune response states. Three differentiation trajectories emerged from unsupervised partitioning (Monocle3, $Q < 0.01$), demonstrating dynamic transition from progenitor-like subpopulations (early pseudotime) to phenotypes with reduced effector function and impaired immune responsiveness (terminal phase) (Figure 7A). This trajectory represents the progressive transition of T cells from an initial progenitor-like state through activation toward a functionally impaired phenotype, reflecting both differentiation and gradual functional deterioration rather than an explicit exhaustion program. T cells in sepsis samples were significantly enriched in the advanced differentiation stage compared to controls and the proportion of advanced cells was significantly increased compared to the normal group (Figure 7B). This indicates that septic T cells accelerate along a trajectory predisposed to dysfunction, whereas control T cells are largely retained in early or intermediate stages, reflecting preserved immune homeostasis.

Longitudinal gene dynamics revealed marked temporal regulation of seven key functional regulators (Figure 7C and D). Further analysis showed that all core genes were significantly down-regulated at the early stage of differentiation (cluster1), a phenomenon that may reflect the dysfunction of T cells in sepsis at the onset of differentiation, which is like a ‘premature power failure of the immune system’, and ultimately leads to the formation of an immunosuppressive microenvironment. Notably, the temporal expression changes of these genes paralleled the pseudotime trajectory, further supporting the interpretation that sepsis drives T cells toward progressively impaired functional states.

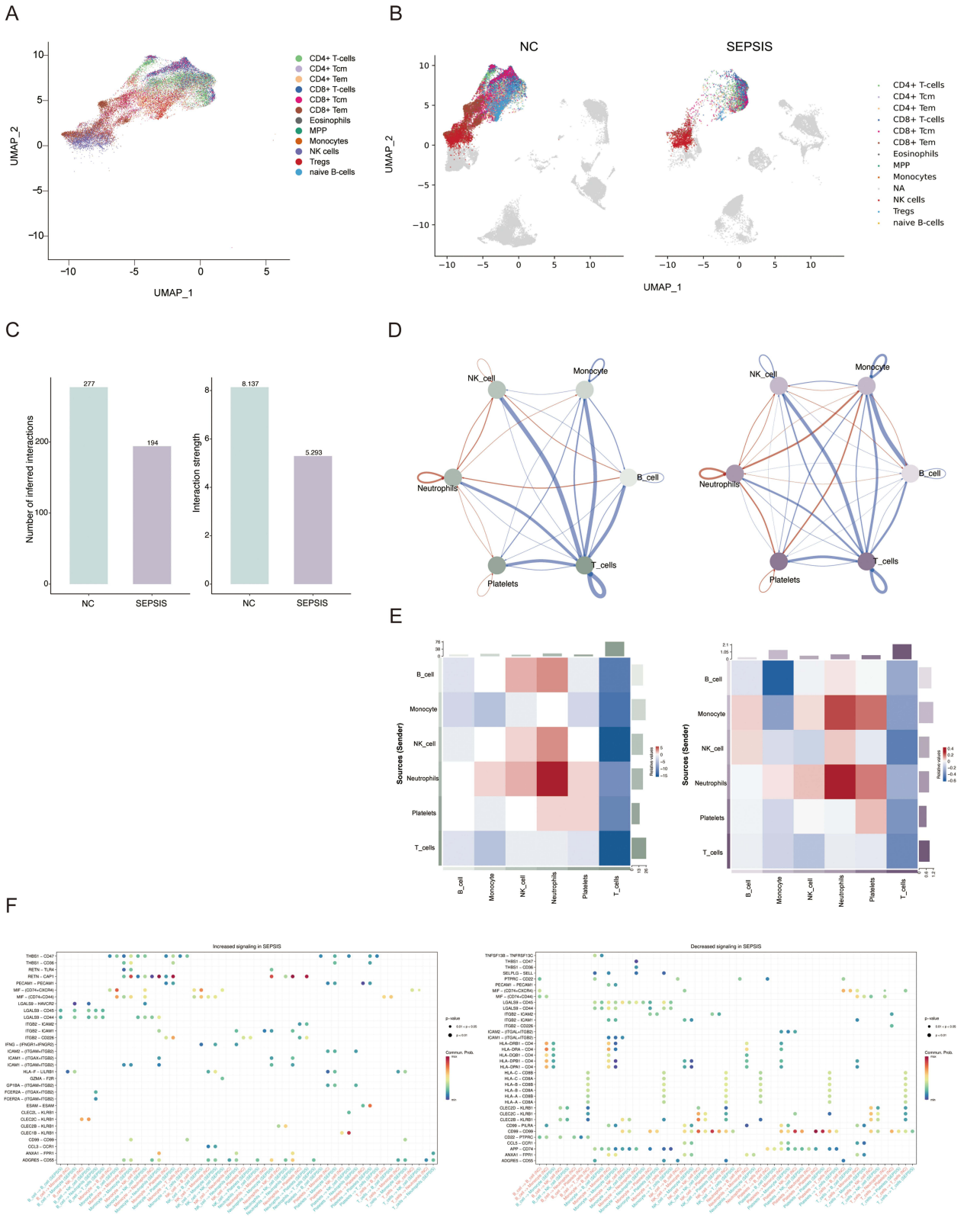

Figure 6 Delineation of T cell subpopulations and analysis of their immune interactions and signaling pathways. (**A**) T-cell Subclustering (12 populations). (**B**) Subpopulation distribution differences (sepsis vs controls). (**C**) Interaction number/intensity histograms (sepsis/normal). (**D**) Interaction networks: green/purple lines indicate sepsis-induced increases/decreases (line thickness = effect magnitude). (**E**) Interaction heatmap: green(decreased) to red (increased). (**F**) Altered ligand-receptor pairs: enhanced (left)/suppressed (right) in sepsis.

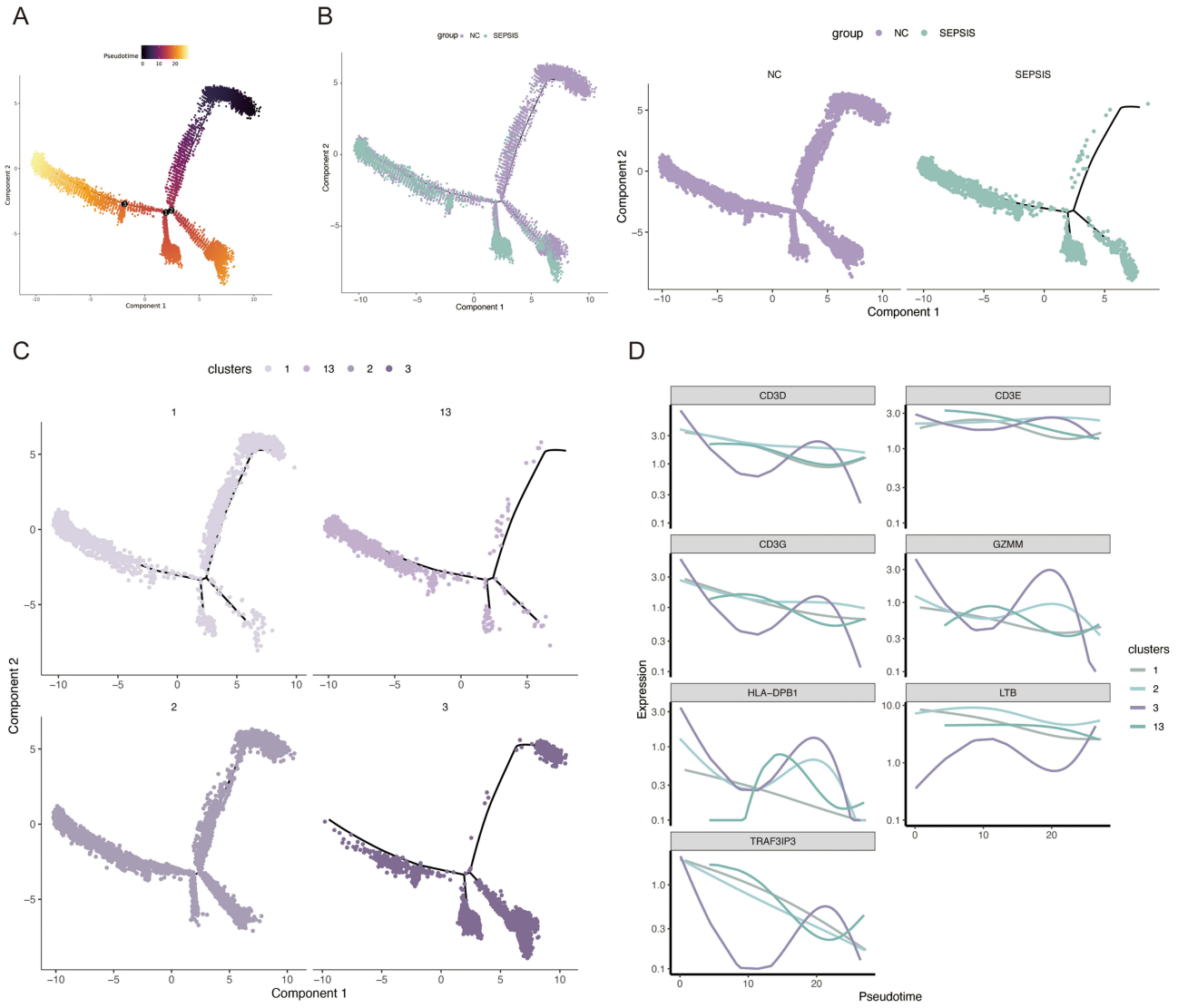

Figure 7 T cell differentiation trajectories and dynamic expression of core genes in sepsis. (**A**) Trajectory diagram of the proposed chronological analysis of T cells, the colors are from dark to light, indicating the time of differentiation from early to late, and each branch represents a biological decision point. (**B**) Group presentation diagram of the proposed chronological trajectory, the purple dots represent the NC team and the light green dots represent the SEPSIS team. T cells in sepsis samples were significantly enriched in the advanced differentiation stage compared to controls, and the proportion of advanced cells was significantly increased compared to the normal group, indicating that septic T cells accelerate toward late dysfunctional states, whereas control T cells are largely retained in early or intermediate stages, reflecting preserved immune homeostasis. (**C**) Diagram of the proposed temporal trajectory of T-cell population differentiation, with each color representing a cell population. (**D**) Plot of proposed temporal expression trend lines of core genes in different subpopulations.

Validation of Diagnostic Performance of Core Genes

Constructing the ROC model based on the GSE95233 validation cohort (sepsis=102, controls=22), all seven candidate genes demonstrated excellent diagnostic performance (Supplementary Figure 2), with the best diagnostic efficacy of *HLA-DPB1* (AUC=0.999), and the best diagnostic efficacy of *CD3E* and *CD3G* (AUC=0.987 and 0.986, respectively) *CD3E* and *CD3G* (AUC=0.987 and 0.986, respectively). The AUC of all the above genes was ≥0.860, and these genes can be used to evaluate and optimize the performance of the prediction model.

Independent Cohort

External validation using an independent cohort (sepsis=22, controls=10) confirmed the conserved downregulation of all seven core genes in sepsis peripheral blood (Figure 8A–G). Differential expression magnitude showed hierarchical significance: T cell receptor (TCR) complex gene *CD3E* exhibited the strongest suppression (p=8.34×10^{-6}), followed by

https://doi.org/10.2147/IDR.S538883

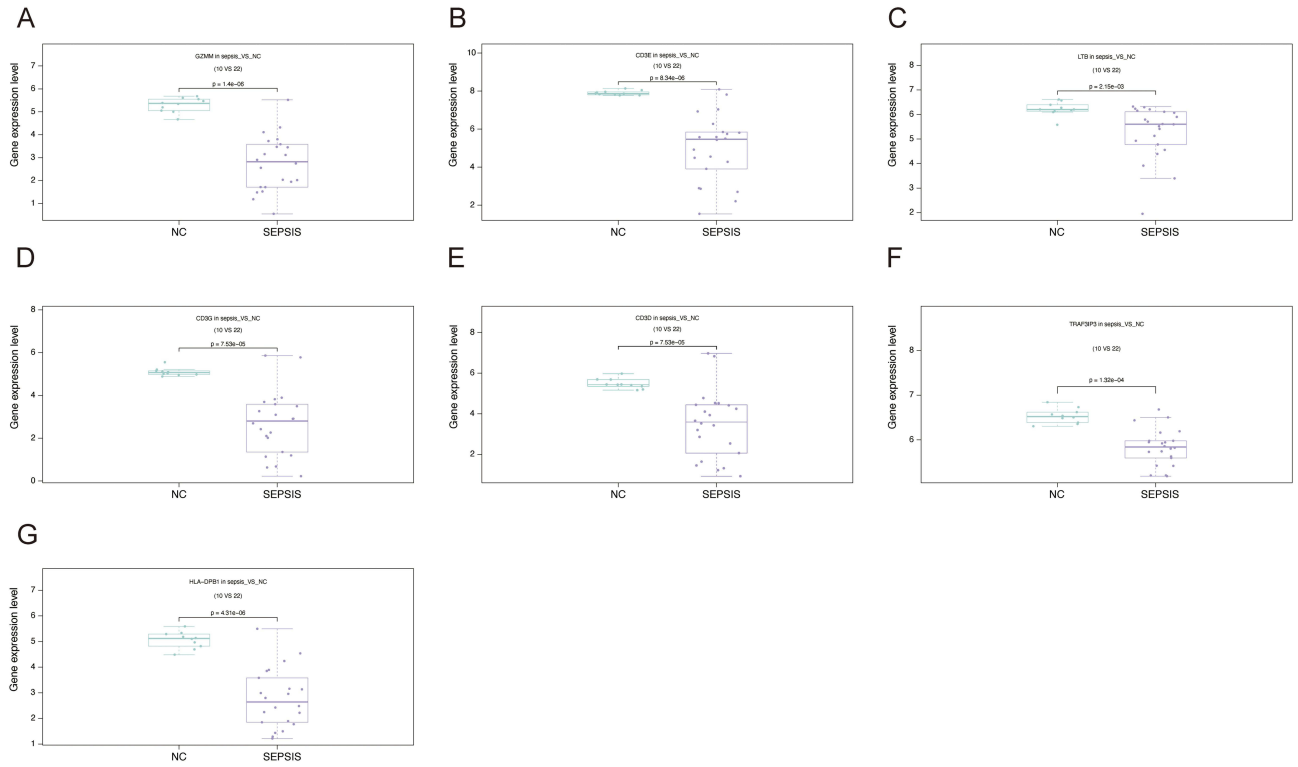

Figure 8 Prospective cohort validation of core gene expression profiles. (**A**–**G**) Bulk RNA-seq expression profiling based on a prospective cohort, demonstrating the gene expression of each core gene in the sepsis group versus the normal group in the transcriptome sequencing data. Light green represents the normal group, and purple represents the sepsis group. The figure shows that all core genes showed consistent down-regulation of expression in the sepsis group, with differences reaching statistical significance ($p < 0.001$).

MHC-II component *HLA-DPB1* (p=4.31×10^{-6}) and cytotoxic granule mediator *GZMM* (p=1.40×10^{-6}). And the consistency of the expression patterns of these core genes validated in independent cohorts further supported their value as potential biomarkers (Supplementary Table 7).

Validation of GEO Datasets

We downloaded four GEO public datasets (GSE232753, GSE69063, GSE185263, GSE100159) and performed grouped box plot visualization with *t*-test analysis of gene expression. The findings indicated significant down-regulation (P<0.05) of seven core genes (*LTB, CD3D, TRAF3IP3, CD3G, GZMM, HLA-DPB1*, and *CD3E*) in sepsis patients relative to healthy controls (Figure 9A–G). This result is consistent with our group's pre-Bulk RNA sequencing data, further supporting the potential role of these genes in sepsis immunosuppression.

All these findings suggest that a multi-omics concordance was established with respect to the transcriptional repression and clinical detectability of *LTB, CD3D, TRAF3IP3, CD3G, GZMM, HLA-DPB1*, and *CD3E*, and that their inhibitory effects may be a common molecular feature of the immunosuppressive state of sepsis.

Prospective Validation of Core Gene Dysregulation and Interaction Network Collapse

To validate the T cell exhaustion mechanisms identified from public datasets at single-cell resolution, this study integrated prospectively generated single-cell transcriptomic data (from 2 sepsis patients [1 survivor, 1 non-survivor] and 2 healthy controls) to verify the cross-platform consistency of expression for seven core genes and the collapse of single-cell communication networks (Figure 10A and B).

Cross-Cohort Validation of Gene Expression Consistency

Consistent with findings from public datasets, all seven core protective genes (eg, *CD3E, LTB, HLA-DPB1*) were significantly downregulated in T cells from sepsis patients ($p < 0.05$). Moreover, the extent of downregulation was

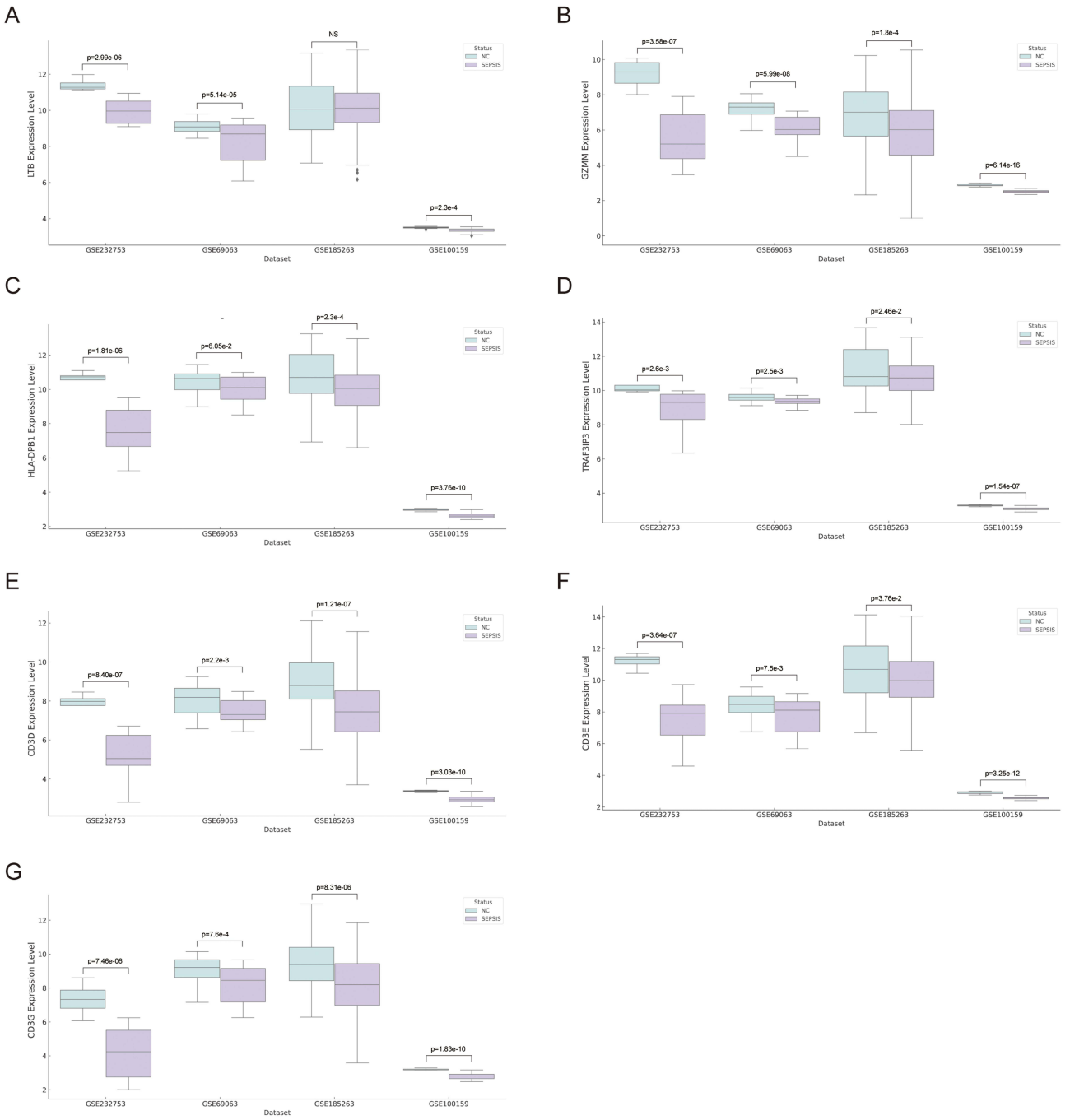

Figure 9 External validation of pivotal genes. (**A**–**G**) Hub gene expression in sepsis group vs control, $P < 0.05$; ns, not significant. (**A**) *LTB*, (**B**) *GZMM*, (**C**) *HLA-DPB1*, (**D**) *TRAF3IP3*, (**E**) *CD3D*, (**F**) *CD3E*, (**G**) *CD3G*.

more pronounced in the non-survivor compared to the survivor (Figure 10C). For instance, the median expression of *LTB* was reduced by 5.9-fold in the non-survivor versus 2.9-fold in the survivor ($p < 0.05$).

Collapse of Cell-Subtype-Specific Immune Interaction Networks

MHC-II signaling collapse: In the non-survivor, *HLA-DRA* expression in $CD4^+$ T cells was significantly reduced ($p < 0.01$), resulting in decreased interaction frequency with antigen-presenting cells (Figure 10D). This is consistent with the inhibition of the MHC-II pathway observed in public datasets. Additionally, reduced interactions such as ITGB2-CD226 and ANXA1-FPR1 (inflammatory resolution axis) suggest the loss of critical immune activation, leading to uncontrolled

https://doi.org/10.2147/IDR.S538883

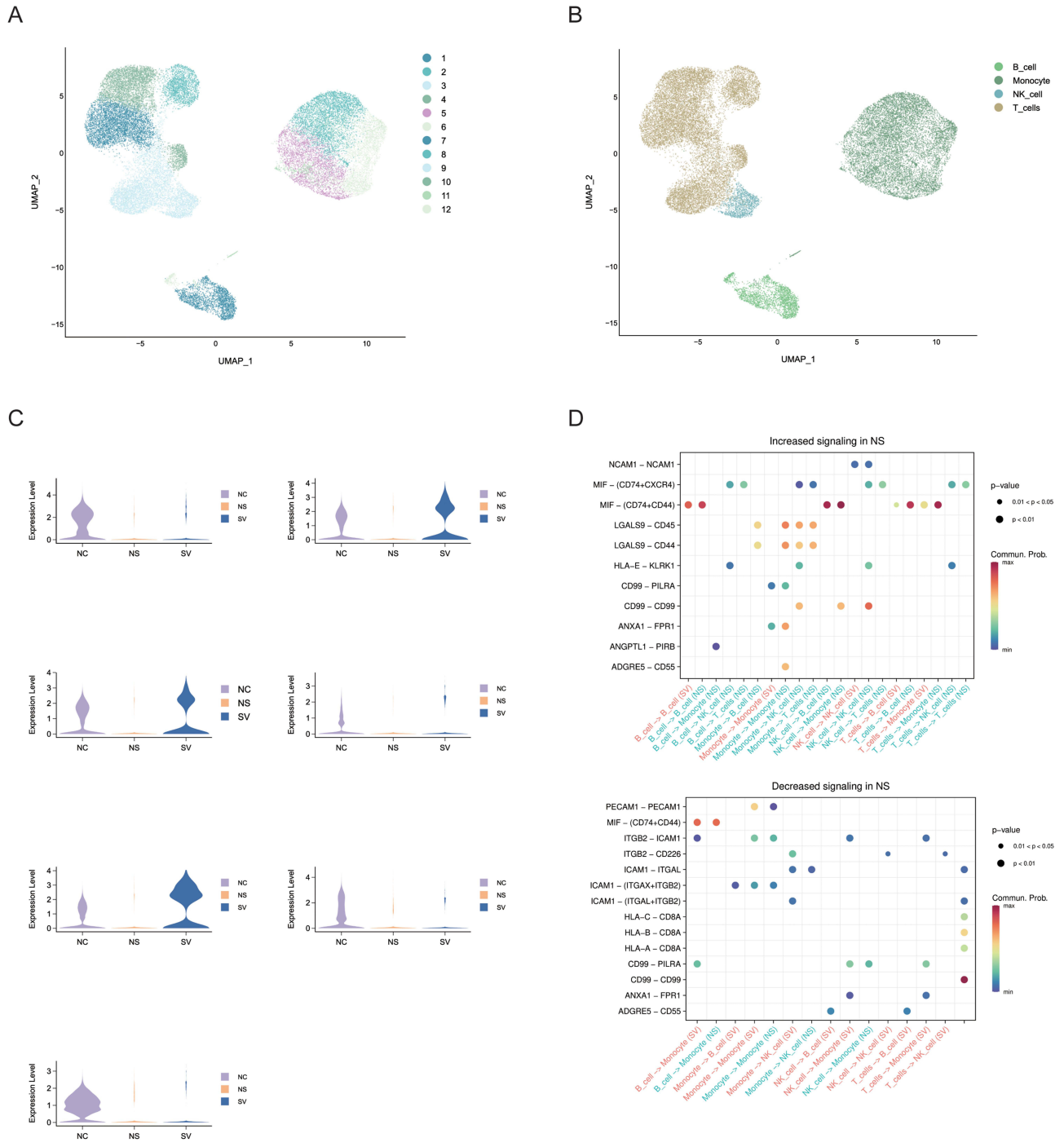

Figure 10 Validation based on prospective single-cell transcriptomic data. (**A**) Single-cell RNA sequencing from the prospective cohort identified 12 distinct cellular clusters. (**B**) Subsequent clustering analysis classified these clusters into four major immune cell types: B cells, monocytes, NK cells, and T cells. (**C**) Violin plots show the expression levels of seven core genes across normal controls (NC), sepsis survivors (SV), and non-survivors (NS). The four genes on the left are *LTB*, *CD3E*, *CD3G*, and *TRAF3IP3* (from top to bottom), while the three genes on the right are *CD3D*, *GZMM*, and *HLA-DPB1* (from top to bottom). (**D**) Alterations in ligand–receptor interactions within T cell subsets between the NS and SV groups. The upper panel shows signaling pathways enhanced in the NS group, while the lower panel shows decreased pathways. Dot size indicates communication probability, and color reflects statistical significance (*p*-value).

inflammation and aggravated tissue damage. Furthermore, enhanced LGALS9-CD45 interaction in the non-survivor indicates a potential driver of T cell exhaustion.

This recurrent synchronous collapse of activation-inhibition-homeostasis suggests that immunotherapy for sepsis may need to move away from traditional checkpoint inhibition strategies to new regimens of targeted reconstructive triple therapy.

Discussion

As a global public health crisis, the pathological complexity of sepsis has led to its high mortality rate (25–30%),[24] and there is an urgent need to break through the limitations of traditional biomarkers (eg, CRP, PCT) in resolving immune heterogeneity. In recent years, breakthroughs in single-cell sequencing technology have provided new opportunities to reveal cell-specific molecular events in sepsis.

Building on this context, our study delineates a continuous chain of evidence to systematically reveal the dynamic mechanisms of T-cell dysfunction in sepsis. Genome-wide GSEA first highlighted a global imbalance of upregulated innate immunity with suppressed T-cell programs, which was further refined by single-cell differential and GO enrichment analyses into key pathways such as TCR signaling and MHC-II antigen presentation. Within this framework, survival analysis of GSE65682 (n=478) identified seven core genes (*LTB*, *CD3D*, *TRAF3IP3*, *CD3G*, *GZMM*, *HLA-DPB1*, *CD3E*) significantly associated with patient survival. These genes were subsequently validated to demonstrate excellent diagnostic efficacy in an independent cohort (AUC $\geq$ 0.86), thereby providing a new direction beyond traditional markers.

The functional heterogeneity of these genes was further clarified by trajectory analysis and interaction mapping. Stable down-regulation of the TCR complex genes (*CD3D*/*CD3E*/*CD3G*) impaired antigen recognition, while suppressive expression of *HLA-DPB1* may exacerbate immunosuppression by modulating Treg activity. In parallel, cellular interaction network analyses revealed a marked reduction in T-cell signaling with NK cells and monocytes, suggesting that disruption of immune synergies is a key driver of immune paralysis in sepsis. Taken together with their cross-subpopulation downregulation and regulatory effects on the immune microenvironment, these genes may serve as novel molecular targets for guiding precision immunotherapy in sepsis.

Consistent with these findings, defects in the function of *HLA-DPB1* in complex with CD3 (CD3D/CD3E/CD3G), a classical immune signaling module, have been widely reported to correlate with T-cell dysfunction. Specifically, *HLA-DPB1* modulates the efficiency of MHC-II antigen presentation and thereby affects Th cell activation,[25–28] while systemic downregulation of the CD3 complex directly impairs TCR signaling, a hallmark of "immune paralysis".[29] Based on this mechanistic background, our work further highlights three relatively underexplored nodes—*LTB, GZMM*, and *TRAF3IP3*—proposing their novel regulatory roles in driving immunosuppression during sepsis:

Immune Microenvironment Regulation by Lymphotoxin β (LTB)

Lymphotoxin β (*LTB*), belonging to the tumor necrosis factor (TNF) superfamily, is essential for regulating adaptive immune responses. It regulates lymphoid organ development, lymphocyte homing and inflammatory microenvironmental homeostasis by forming a heterotrimeric complex with lymphotoxin α (LTα), binding to the LTβ receptor (LTβR) and activating the NF-κB signalling pathway.[30] Notably, the *LTB-LTβR* axis is critical for the development of follicular helper T cells (Tfh) and regulatory T cells (Treg) - reductions in Tfh and Treg in LTβR-deficient patients directly contribute to dysregulation of humoral immunity and imbalance of autoimmune tolerance.[31] Analysis of single-cell interactions showed that the intensity of *LTB-LTβR* interactions between LTB+ T cells and monocytes was significantly reduced in sepsis, suggesting that a break in their mediated immune synergy may be a key trigger for the imbalance in the immune microenvironment. This phenomenon may exacerbate immunosuppression through a dual mechanism: i) destruction of lymphoid structures: downregulation of *LTB* may lead to impeded formation of high endothelial microvessels (HEVs) in secondary lymphoid organs, impairing T/B cell synergy and pathogen clearance; ii) imbalance in the regulation of inflammation: the absence of *LTB-LTβR* signalling may reduce the secretion of chemokines, such as CXCL13, by stromal cells, and inhibit the neutrophilic granulocyte extracellular traps (NETs) clearance, exacerbating tissue damage.[32,33] Future studies need to validate the function of *LTB* in sepsis through gene editing models and explore the therapeutic potential of targeting the LTβR pathway to restore immune homeostasis.

Cytotoxic Remodelling of Granzyme M (GZMM)

Granzyme M (*GZMM*), a member of the granzyme family, is a central effector molecule in cytotoxic T cells and natural killer cells (NK cells) mediated immunocide. It enters target cells through a perforin-dependent pathway, specifically cleaves substrates (eg, proteasome subunit PSME2), activates caspase-independent cell death pathways, and plays

a unique role in anti-infection and tumour immune surveillance.[34] Although *GZMM* is expressed at lower levels than other granzymes (eg GZMB), its role in certain immune responses and tumour immunosurveillance is irreplaceable. In the present study, *LTB* expression was significantly down-regulated in the peripheral blood and single-cell transcriptome of sepsis patients, and its low expression was significantly associated with 28-day mortality. Single-cell interaction analysis further showed that the intensity of granzyme-perforin signalling flow between GZMM+ T cells and target cells (eg infected monocytes) was reduced in sepsis, suggesting impaired immune synapse function. Thus, *GZMM* may lead to delayed pathogen clearance and immune escape through: i) defective cytotoxic function: down-regulation of *GZMM* weakens the direct killing capacity of CD8+ T cells and NK cells;[35] (ii) Imbalance of inflammatory regulation: *GZMM* regulates the intensity of inflammatory response through cleavage of inflammation-related proteins (eg IL-1β precursor),[36] and inhibition of its expression may exacerbate the "cytokine storm" and tissue damage in sepsis; (iii) Dysregulation of TCR signalling feedback: the *GZMM* is involved in the negative feedback regulation of the TCR signalling pathway,[37] and its absence may lead to accelerated T-cell overactivation or depletion. Based on this, future conditional knockout models need to be constructed to validate the causal association of *GZMM* deficiency on sepsis prognosis and to explore the therapeutic potential of recombinant *GZMM* proteins or agonists.

TRAF3IP3-Mediated Immunometabolic Imbalance

TRAF3IP3 (an interacting protein of TNF receptor-associated factor 3) is a novel immunomodulatory molecule that plays a pleiotropic role in the development and function of adaptive immunity by modulating the TRAF3-mediated signalling network. It maintains metabolic adaptation of regulatory T cells (Treg) through lysosomal localization and drives Th17 cell differentiation, thereby balancing anti-microbial immunity and autoimmune tolerance.[38,39] Zou et al demonstrated that *TRAF3IP3* promotes thymocyte-positive selection through activation of the ERK signalling pathway, and that its absence leads to reduced mature T cell production and an imbalance in peripheral T cell homeostasis.[40] Based on the previous studies, the significant down-regulation of *TRAF3IP3* in single-cell sequencing analysis and transcriptomics may exacerbate sepsis immunosuppression through the following mechanisms: i) Treg failure: down-regulation of *TRAF3IP3* may disrupt the lysosomal metabolic homeostasis of Tregs, leading to impaired immune-suppressive function and inability to effectively inhibit excessive inflammatory responses;[41] (ii) Th17/Treg imbalance: *TRAF3IP3* deficiency inhibits Th17 differentiation, weakening intracellular pathogen immunity and exacerbating Treg dysfunction, resulting in a vicious cycle of "low immunity-high inflammation";[42] (iii) ERK signalling disruption: *TRAF3IP3*-mediated inhibition of ERK signalling may block key pathways of T-cell activation and proliferation, accelerating T-cell depletion.[39] In addition, single-cell interaction analysis showed that the intensity of CD86-CTLA4 interactions between TRAF3IP3+ Treg and monocytes was reduced in sepsis, suggesting that disruption of the immune checkpoint signalling it regulates may weaken the stability of the immunosuppressive microenvironment. Notably, differentiation trajectory analysis showed that *TRAF3IP3* was consistently downregulated early in T cell differentiation (Figure 10D) and may act as an early driver of T cell depletion.

Previous studies have primarily focused on phenotypic features of T cell exhaustion in sepsis, such as PD-1 upregulation;[13] however, the gene regulatory networks and intercellular crosstalk mechanisms driving this process remain poorly understood. In contrast to prior studies relying solely on public databases, we innovatively integrated prospective in-house sequencing data with multi-platform validation strategies, establishing for the first time the functional loss of TCR complex genes (*CD3D*/*CD3E*) and MHC-II molecules (eg, *HLA-DPB1*) as critical contributors to the dynamic progression of immunosuppression in sepsis. For instance, in our prospective cohort, non-survivors exhibited a 5.9-fold decrease in *CD3E* expression compared to survivors ($p<0.05$), accompanied by significantly exacerbated collapse of monocyte interactions (HLA-DRA-MHCII pathway) ($p=0.007$). This finding mechanistically complements the T cell phenotypic remodeling reported by Reyes et al,[12] elucidating the molecular basis of phenotypic heterogeneity at the gene regulatory level.

Notably, our cross-omics interaction network analysis transcends the limitations of conventional approaches: We not only identified ITGB2-CD226 signaling deficiency as a core mechanism underlying impaired T cell co-stimulation in sepsis (48% reduction in pathway activity in non-survivors vs survivors, $p=0.008$) but also revealed that aberrant activation of the LGALS9-CD45 pathway drives immune exhaustion by suppressing TCR phosphorylation (72% reduction in $CD3E^{+}$ cells via single-cell trajectory analysis). This dual imbalance of "co-stimulation inhibition–

checkpoint activation" suggests that restoring HLA-DRA-MHCII antigen presentation or blocking LGALS9-CD45 inhibitory signaling may reverse T-cell dysfunction or exhaustion-like states, offering a novel therapeutic direction beyond traditional targets like PD-1/CTLA-4. Of particular translational relevance, *CD3E*—a core component of the TCR complex—exhibited the strongest survival association (HR=4.50), positioning it as a priority target for therapeutic antibodies or gene-editing strategies.

Limitations and Future Directions

Although our cross-platform validation confirmed the conservation of core genes, several limitations should be acknowledged: (1) The modest sample size, particularly in the prospective scRNA-seq cohort, may limit statistical power for rare cell subsets; (2) Survival analyses were based on retrospective data, necessitating validation in prospective clinical trials; (3) Functional mechanisms of core genes (eg, CD3D-mediated regulation of T cell activation) remain experimentally unverified. Future studies should employ sepsis murine models to validate gene functions and explore targeted interventions, such as CD3E agonists. Additionally, although our analyses indicate profound T-cell dysfunction, we did not directly assess classical exhaustion markers such as PD-1, which should be included in future studies to more precisely define the exhaustion phenotype.

Conclusion

This study unveils the core gene networks and intercellular communication collapse driving T cell dysfunction in sepsis through integrated multi-omics analysis, while validating their diagnostic and prognostic utility. These findings establish a theoretical foundation for precision therapies targeting T cell functional remodeling and provide novel biomarkers for immune monitoring in sepsis.

Abbreviations

Treg, Regulatory T cells; scRNA-seq, Single-cell RNA sequencing; IFNG, Interferon Gamma; GEO, Gene Expression Omnibus; QC, Quality Control; UMI, Unique Molecular Identifier; UMAP, Uniform Manifold Approximation and Projection; GO, Gene Ontology; GSEA, Gene Set Enrichment Analysis; AUC, Area Under the Curve; ROC, Receiver Operating Characteristic; MHC, Major Histocompatibility Complex; TCR, T-cell Receptor; MST, Minimum Spanning Tree.

Data Sharing Statement

The autosequencing raw data are stored in the National Genebank of China database (CNGBdb), which can be accessed via specific links and login numbers in the Methods section or requested from the corresponding author YCH. The data generated and analyzed during the current study are available in the Supplementary Information File, which provides detailed descriptions of the analytical process, as well as the corresponding Supplementary Figures and Tables with legends.

Acknowledgments

We thank OEBIOTECH for guidance on scRNA-seq and Vecteezy (http://www.vecteezy.com) online platform for graphical abstract material.

Author Contributions

All authors made a significant contribution to the work reported, whether that is in the conception, study design, execution, acquisition of data, analysis and interpretation, or in all these areas; took part in drafting, revising or critically reviewing the article; gave final approval of the version to be published; have agreed on the journal to which the article has been submitted; and agree to be accountable for all aspects of the work.

Funding

Funding for this study was provided by the Collaborative Project of the Affiliated Hospital of Southwest Medical University in Luzhou City (Grant 2024LZXNYDJ038) and the Sichuan Provincial Clinical Key Speciality Project (Grant 23LCYJ001).

Disclosure

All authors declares no conflict of interest.

References

1. Meyer NJ, Prescott HC. Sepsis and Septic Shock. *New Engl J Med*. 2024;391(22):2133–2146. doi:10.1056/NEJMra2403213
2. Rudd KE, Johnson SC, Agesa KM, et al. Global, regional, and national sepsis incidence and mortality, 1990–2017: analysis for the Global Burden of Disease Study. *Lancet*. 2020;395(10219):200–211. doi:10.1016/S0140-6736(19)32989-7
3. Cajander S, Kox M, Scicluna BP, et al. Profiling the dysregulated immune response in sepsis: overcoming challenges to achieve the goal of precision medicine. *Lancet Resp Med*. 2023;12(4):305–322. doi:10.1016/S2213-2600(23)00330-2
4. El-Khazragy N, Mohamed NM, Mostafa MF, et al. miRNAs: novel noninvasive biomarkers as diagnostic and prognostic tools in neonatal sepsis. *Diagnostic Microbiol Infect Dis*. 2023;107(3):116053. doi:10.1016/j.diagmicrobio.2023.116053
5. Jiang Y, Rosborough BR, Chen J, et al. Single cell RNA sequencing identifies an early monocyte gene signature in acute respiratory distress syndrome. *JCI Insight*. 2020;5(13):e135678. doi:10.1172/jci.insight.135678
6. Yao RQ, Li ZX, Wang LX, et al. Single-cell transcriptome profiling of the immune space-time landscape reveals dendritic cell regulatory program in polymicrobial sepsis. *Theranostics*. 2022;12(10):4606–4628. doi:10.7150/thno.72760
7. Zhang W, Wang Z. Zhonghua wei Zhong Bing ji jiu yi xue. *Zhonghua wei Zhong Bing ji jiu yi xue*. 2022;34(1):95–99. doi:10.3760/cma.j.cn121430-20210610-00858
8. Kaufmann I, Hoelzl A, Schliephake F, et al. Polymorphonuclear leukocyte dysfunction syndrome in patients with increasing sepsis severity. *Shock*. 2006;26(3):254–261. doi:10.1097/01.shk.0000223131.64512.7a
9. Ding S, Chen X, Shen K. Single-cell RNA sequencing in breast cancer: understanding tumor heterogeneity and paving roads to individualized therapy. *Cancer Commun*. 2020;40(8):329–344. doi:10.1002/cac2.12078
10. Su M, Pan T, Chen QZ, et al. Data analysis guidelines for single-cell RNA-seq in biomedical studies and clinical applications. *Military Med Res*. 2022;9(1):68. doi:10.1186/s40779-022-00434-8
11. Zhao M, Jiang J, Zhao M, Chang C, Wu H, Lu Q. The Application of Single-Cell RNA Sequencing in Studies of Autoimmune Diseases: a Comprehensive Review. *Clin Rev Allergy Immunol*. 2021;60(1):68–86. doi:10.1007/s12016-020-08813-6
12. Reyes M, Filbin MR, Bhattacharyya RP, et al. An immune-cell signature of bacterial sepsis. *Nature Med*. 2020;26(3):333–340. doi:10.1038/s41591-020-0752-4
13. Menges T, Engel J, Welters I, et al. Changes in blood lymphocyte populations after multiple trauma: association with posttraumatic complications. *Crit Care Med*. 1999;27(4):733–740. doi:10.1097/00003246-199904000-00026
14. Wilson JK, Zhao Y, Singer M, Spencer J, Shankar-Hari M. Lymphocyte subset expression and serum concentrations of PD-1/PD-L1 in sepsis - pilot study. *Crit Care*. 2018;22(1):95. doi:10.1186/s13054-018-2020-2
15. Shen YZ, Xiong W, Hu YC, Zhong W. SPP1 is a plasma biomarker associated with the dia gnosis and prediction of prognosis in sepsis. *Sci Rep*. 2024;14(1):27205. doi:10.1038/s41598-024-78420-4
16. Li S, Shen Y, Wang C, Yang J, Chen M, Hu Y. Exploring the prognostic and diagnostic value of lactylation-related genes in sepsis. *Sci Rep*. 2024;14(1):23130. doi:10.1038/s41598-024-74040-0
17. Wang C, Li Y, Li S, Chen M, Hu Y. Proteomics Combined with RNA Sequencing to Screen Biomarkers of Sepsis. *Infect Drug Resist*. 2022;15:5575–5587. doi:10.2147/IDR.S380137
18. Gordon JAR, Evans MF, Ghule PN, et al. Identification of molecularly unique tumor-associated mesenchymal stromal cells in breast cancer patients. *PLoS One*. 2023;18(3):e0282473. doi:10.1371/journal.pone.0282473
19. 10x Genomics. (2021). Cell Ranger Software Documentation. Available from: https://support.10xgenomics.com/single-cell-gene-expression/software. Accessed Sep 9, 2025.
20. Jin S, Guerrero-Juarez CF, Zhang L, et al. Inference and analysis of cell-cell communication using CellChat. *Nat Commun*. 2021;12(1):1088. doi:10.1038/s41467-021-21246-9
21. Yao RQ, Zhao PY, Li ZX, et al. Single-cell transcriptome profiling of sepsis identifies HLA-DRlowS100Ahigh monocytes with immunosuppressive function. *Military Medical Research*. 2023;10(1):27. doi:10.1186/s40779-023-00462-y
22. Trapnell C, Cacchiarelli D, Grimsby J, et al. The dynamics and regulators of cell fate decisions are revealed by pseudotemporal ordering of single cells. *Nature Biotechnology*. 2014;32(4):381–386. doi:10.1038/nbt.2859
23. Korsunsky I, Millard N, Fan J, et al. Fast, sensitive and accurate integration of single-cell data with Harmony. *Nat Methods*. 2019;16(12):1289–1296. doi:10.1038/s41592-019-0619-0
24. Minasyan H. Sepsis: mechanisms of bacterial injury to the patient. *Scand J Trauma Resusc Emerg Med*. 2019;27(1):19. doi:10.1186/s13049-019-0596-4
25. Mohsin M, Singh P, Khan S, et al. Integrated transcriptomic and regulatory network analyses uncovers the role of let-7b-5p, SPIB, and HLA-DPB1 in sepsis. *Sci Rep*. 2022;12(1). doi:10.1038/s41598-022-16183-6
26. Choo SY. The HLA system: genetics, immunology, clinical testing, and clinical implications. *Yonsei Med J*. 2007;48(1):11–23. doi:10.3349/ymj.2007.48.1.11
27. Nudel R, Allesøe RL, Thompson WK, Werge T, Rasmussen S, Benros ME. A large-scale investigation into the role of classical HLA loci in multiple types of severe infections, with a focus on overlaps with autoimmune and mental disorders. *J Transl Med*. 2021;19(1). doi:10.1186/s12967-021-02888-1
28. Tian C, Hromatka BS, Kiefer AK, et al. Genome-wide association and HLA region fine-mapping studies identify susceptibility loci for multiple common infections. *Nat Commun*. 2017;8(1):599. doi:10.1038/s41467-017-00257-5
29. Heffernan DS, Monaghan SF, Thakkar RK, Machan JT, Cioffi WG, Ayala A. Failure to normalize lymphopenia following trauma is associated with increased mortality, independent of the leukocytosis pattern. *Critical Care*. 2012;16(1):R12. doi:10.1186/cc11157
30. Junt T, Tumanov AV, Harris N, et al. Expression of lymphotoxin beta governs immunity at two distinct levels. *European Journal of Immunology*. 2006;36(8):2061–2075. doi:10.1002/eji.200626255
31. Ransmayr B, Bal SK, Thian M, et al. LTβR deficiency causes lymph node aplasia and impaired B cell differentiation. *Sci Immunol*. 2024;9(101):eadq8796. doi:10.1126/sciimmunol.adq8796

32. Hua Y, Vella G, Rambow F, et al. Cancer immunotherapies transition endothelial cells into HEVs that generate TCF1+ T lymphocyte niches through a feed-forward loop. *CANCER CELL*. 2022;40(12):1600–1618.e10. doi:10.1016/j.ccell.2022.11.002
33. Ansel KM, Ngo VN, Hyman PL, et al. A chemokine-driven positive feedback loop organizes lymphoid follicles. *Nature*. 2000;406(6793):309–314. doi:10.1038/35018581
34. Trapani JA. Granzymes: a family of lymphocyte granule serine proteases. *Genome Biol*. 2001;2(12):3014. doi:10.1186/gb-2001-2-12-reviews3014
35. Pao LI, Sumaria N, Kelly JM, et al. Functional analysis of granzyme M and its role in immunity to infection. *J Immunol*. 2005;175(5):3235–3243. doi:10.4049/jimmunol.175.5.3235
36. Kuechler PC, Britschgi M, Schmid S, Hari Y, Grabscheid B, Pichler WJ. Cytotoxic mechanisms in different forms of T-cell-mediated drug allergies. *ALLERGY*. 2004;59(6):613–622. doi:10.1111/j.1398-9995.2004.00460.x
37. Kalia V, Penny LA, Yuzefpolskiy Y, Baumann FM, Sarkar S. Quiescence of Memory CD8(+) T Cells Is Mediated by Regulatory T Cells through Inhibitory Receptor CTLA-4. *Immunity*. 2015;42(6):1116–1129. doi:10.1016/j.immuni.2015.05.023
38. Deng M, Tam JW, Wang L, et al. TRAF3IP3 negatively regulates cytosolic RNA induced anti-viral signaling by promoting TBK1 K48 ubiquitination. *Nat Commun*. 2020;11(1). doi:10.1038/s41467-020-16014-0
39. Yu X, Teng XL, Wang F, et al. Metabolic control of regulatory T cell stability and function by TRAF3IP3 at the lysosome. *J Exp Med*. 2018;215 (9):2463–2476. doi:10.1084/jem.20180397
40. Zou Q, Jin J, Xiao Y, et al. T cell development involves TRAF3IP3-mediated ERK signaling in the Golgi. *J Exp Med*. 2015;212(8):1323–1336. doi:10.1084/jem.20150110
41. Li H, Yao Y, Zhang S, Deng Z, Qiao W, Tan J. TRAF3IP3 Is Cleaved by EV71 3C Protease and Exhibits Antiviral Activity. *Front Microbiol*. 2022;13:914971. doi:10.3389/fmicb.2022.914971
42. Zhang X, Wang K, Zhao W, et al. TRAF3IP3 at the trans-Golgi network regulates NKT2 maturation via the MEK/ERK signaling pathway. *Cell Mol Immunol*. 2020;17(4):395–406. doi:10.1038/s41423-019-0234-0